Coarse-grained simulation of chaotic mixing in laminar flows

A. Vikhansky*
Department of Engineering, Queen Mary, University of London, Mile End Road, London E1 4NS, United Kingdom
(Received 24 January 2006; published 23 May 2006)

A model for chaotic mixing has been formulated and tested. The advection of a passive scalar by laminar flows with high Péclet numbers is modeled by a finite-volume method on a coarse grid. The scales which are smaller than the increment of the grid are modeled by an approximate subgrid model. The artificial diffusivity of the finite-difference method plays a twofold role. It prevents the formation of spurious oscillations of the solution and also models the transport of the variation of the scalar from the large to subgrid modes.

DOI: 10.1103/PhysRevE.73.056707 PACS number(s): 47.11.−j, 47.51.+a, 47.15.−x, 47.52.+j

I. INTRODUCTION

In this paper we consider the mixing of a passive scalar, with coefficient of diffusion D, by a laminar flow. If the substance is carried by an incompressible flowfield $u_k(t,x_l)$ with characteristic length L and characteristic velocity U, the dimensionless advection-diffusion equation of the process reads

$$\frac{\partial C}{\partial t}+u_k\frac{\partial C}{\partial x_k}-\frac{1}{\mathrm{Pe}}\frac{\partial^2 C}{\partial x_k^2}=0, \tag{1}$$

where $C(t,x_l)$ is the concentration and $\mathrm{Pe}=LU/D$ is the Péclet number. Multiplying Eq. (1) by C yields, after some algebra, the following equation for the scalar variance:

$$\frac{\partial C^2}{\partial t}+u_k\frac{\partial C^2}{\partial x_k}-\frac{1}{\mathrm{Pe}}\frac{\partial^2 C^2}{\partial x_k^2}=-\frac{2}{\mathrm{Pe}}\left(\frac{\partial C}{\partial x_k}\right)^2, \tag{2}$$

i.e., the variance decreases due to the diffusivity until the system reaches a spatially uniform state. If diffusivity is low, i.e., $\mathrm{Pe}\gg 1$ the mixing is slow unless it is enhanced by an appropriate flowfield. The route to effective mixing is then a chaotic flow; such flows have, over the last 20 years or so, been shown to provide the paradigm for effective mixing at small scales [1–4].

The main features of the laminar mixing at high Pe are captured by the so-called "lamellar" model [5–12]. At the initial stages of chaotic mixing, the streams to be mixed are advected and stretched by the flow and the interface between the components grows exponentially with time. A complicated structure of thin striations of the components then emerges in the mixing zone. Since the flow is incompressible, stretching in one direction means contraction in at least one other direction; the striation thickness and separation decrease, until diffusion smooths out the deviations of the concentration. Although the lamellar model captures the essential physics of the process, it also predicts a very fast superexponential decay of the variations of the scalar. Since Eq. (1) is a linear one, the concentration field C can be represented as a linear combination of noninteracting modes. These so-called "strange" modes decay exponentially as the concentration field approaches the fully mixed state. Thiffeault [11] considered the strange eigenmodes in Lagrangian coordinates; it was shown that the lamellar model becomes invalid when the gradients along the stable direction become smaller than the gradients in the orthogonal direction.

The numerical solution of Eq. (1) with high Pe is almost as time-consuming as a direct numerical simulation of a turbulent flow with high Re. The similarity between chaotic advection and turbulence has an important implication. Although no universal theory of turbulence has ever been formulated, the decades-long experience of turbulence modeling says that numerous empirical, semiempirical, and analytical models based on different types of closure assumptions can be and have to be formulated [13–15].

In the present investigation we consider a numerical method for simulation of laminar mixing on a coarse grid. The large scales of the concentration field are resolved by a finite-volume method. A closure assumption is used to account for the subgrid scales. The proposed model, although it cannot be derived from first principles, captures the two main features of the chaotic mixing, namely, lamellar structure of the concentration field and exponential decay of the variations of the scalar. A similar approach, i.e., direct tracking at large scales together with an approximate modeling of the subgrid scales has been used in Ref. [16] to simulate evolution of a passive interface between two immiscible liquids with identical mechanical properties.

II. THE MODEL

In order to get rid of the scales less than the grid spacing Δx we use the same idea which was successfully used in large-eddy simulations of turbulent flows [13,14]. Let us define a filter operator which acts on a function f as

$$\bar{f}(\boldsymbol{x})=\frac{1}{h^d}\int_\Omega \mathcal{F}\left(\frac{\boldsymbol{y}-\boldsymbol{x}}{h}\right)f(\boldsymbol{y})d\boldsymbol{y}, \tag{3}$$

where the averaging is performed over a region with a characteristic size h, d is the dimension of the space, and the function $\mathcal{F}$ satisfies the following conditions: (i) $\mathcal{F}(z)\geqslant 0$; (ii) $\int_\Omega \mathcal{F}(z)dz=1$.

Even if the initial conditions of Eq. (1) are smooth enough, the flow field sharpens the gradients of the solution. Therefore, the filter operation has to be applied to $\overline{C(t,x_l)}$

*Electronic address: a.vikhansky@qmul.ac.uk

after every time interval Δt in order to keep the concentration field smooth. Since the filtration spreads every perturbation over a region of order h, the effect of filtration is similar to a diffusion with diffusivity coefficient $D \sim h^2/\Delta t$. Thus, we postulate that $\overline{C(t,x_l)}$ satisfies the following equation:

$$\frac{\partial \bar{C}}{\partial t} + u_k \frac{\partial \bar{C}}{\partial x_k} - \frac{1}{\mathrm{Pe}} \frac{\partial^2 \bar{C}}{\partial x_k^2} = \frac{\partial}{\partial x_m}\left(\mathcal{D}_{mn} \frac{\partial \bar{C}}{\partial x_n}\right), \tag{4}$$

where $\mathcal{D}_{mn}$ is the artificial (anisotropic) diffusivity which will be specified below. In the above equation we assume that the characteristic scale of the flowfield is bigger than h and

$$\overline{u_k(t,x_l)} = u_k(t,x_l), \quad \overline{u_k(t,x_l)C(t,x_l)} = u_k(t,x_l)\overline{C(t,x_l)}.$$

Note that in the large-eddy simulation of turbulent flows the turbulent viscosity is accounting for a real physical process, i.e., momentum transport by small eddies. In the present model the artificial diffusivity is introduced because the scales smaller than the grid increment Δx of our finite-volume method cannot be resolved properly. The artificial diffusivity does not represent any physical process and introduces an error which decreases as Δx and h get smaller.

Let us split the concentration field into filtered and fluctuating parts

$$C(t,x_l) = \overline{C(t,x_l)} + c(t,x_l), \tag{5}$$

where $\overline{c(t,x_l)}=0$ and $\overline{C(t,x_l)c(t,x_l)}=0$. Substitution of Eq. (5) into Eq. (2) yields two uncoupled equations for C^2 and c^2, respectively. At this point we make our first approximation. The additional diffusive term in Eq. (4) is due to the filtration of the concentration field and the variation of the concentration which is dissipated by the artificial diffusion has to appear at the subgrid level. Therefore we postulate an equation for $\overline{c^2}$ of the following form:

$$\frac{\partial \overline{c^2}}{\partial t} + u_k \frac{\partial \overline{c^2}}{\partial x_k} - \frac{1}{\mathrm{Pe}} \frac{\partial^2 \overline{c^2}}{\partial x_k^2} = -\frac{2}{\mathrm{Pe}} A_{kk} + 2\mathcal{D}_{mn} \frac{\partial \bar{C}}{\partial x_m} \frac{\partial \bar{C}}{\partial x_n}, \tag{6}$$

where $A_{ij} = \overline{\partial c/\partial x_i \, \partial c/\partial x_j}$ and the last term shows how fast the variation of the scalar is transported from the large to the subgrid unresolved scales.

In order to obtain an equation for the tensor A_{ij} we apply the operator

$$\frac{\partial C}{\partial x_i}\frac{\partial}{\partial x_j} + \frac{\partial C}{\partial x_j}\frac{\partial}{\partial x_i}$$

to Eq. (1). As in Eq. (6) the dissipation at the large scales serves as a source at the subgrid scales and the equation for A_{ij} reads

$$\frac{\partial A_{ij}}{\partial t} + u_k \frac{\partial A_{ij}}{\partial x_k} + \frac{\partial u_k}{\partial x_i} A_{kj} + A_{ik} \frac{\partial u_k}{\partial x_j} - \frac{1}{\mathrm{Pe}} \frac{\partial^2 A_{ij}}{\partial x_k^2} = -\frac{2}{\mathrm{Pe}} B_{ikkj} + \dot{S}_{ij}, \tag{7}$$

where $B_{ijkl} = \overline{(\partial^2 c/\partial x_i \partial x_j)(\partial^2 c/\partial x_k \partial x_l)}$ and $\dot{S}_{ij}$ are the dissipation and the production terms, respectively.

The production term $\dot{S}_{ij}$ must satisfy the following conditions: (i) it has to be collinear to $\partial \bar{C}/\partial x_i \partial \bar{C}/\partial x_j$, i.e., the subgrid interface is parallel to the coarse-grained one; (ii) it has to be proportional to the production term in Eq. (6); (iii) the characteristic scale of $\dot{S}_{ij}$ is Δx. Combining these conditions yields

$$\dot{S}_{ij} = \frac{2\mathcal{D}_{mn}}{(\Delta x)^2}\left(\frac{\partial \bar{C}}{\partial x_m}\frac{\partial \bar{C}}{\partial x_n}\right)\left(\frac{\partial \bar{C}}{\partial x_i}\frac{\partial \bar{C}}{\partial x_j}\right)\left(\frac{\partial \bar{C}}{\partial x_k}\right)^{-2}. \tag{8}$$

Note that in a chaotic flow, the principal axis and growth rate of A_{ij} reach their asymptotic values exponentially fast. Thus, $\dot{S}_{ij}$ is only an "ignition spark" and its form does not really affect the outcome of the calculations.

In the present investigation we use the following closure approximation for the dissipation rate of the subgrid gradients which follows from dimensional arguments

$$B_{ikkj} = (1+\beta)\frac{A_{kk}}{\overline{c^2}} A_{ij}, \tag{9}$$

where β is a parameter. In order to elucidate the meaning of Eq. (9) let us consider a zero-dimensional counterpart of Eqs. (4), (6), (7), and (9). A spatially uniform (at large scales) lamellar structure which is stretched with a constant rate λ is characterized by the single component $A_{11}=A$. Thus, the Eqs. (6) and (7) read

$$\frac{d\overline{c^2}}{dt} = -\frac{2}{\mathrm{Pe}} A, \quad \frac{dA}{dt} = 2\lambda A - \frac{2(1+\beta)}{\mathrm{Pe}} \frac{A^2}{\overline{c^2}}. \tag{10}$$

Initially $\overline{c^2}$ does not change (if $\mathrm{Pe} \gg 1$), while A grows with exponent 2λ and the characteristic striation thickness $\delta \sim (\overline{c^2}/A)^{1/2}$ decreases with the exponent $-\lambda$. At time $t_* \sim \lambda^{-1} \ln(\lambda \mathrm{Pe}/\beta)$ when A becomes high enough, Eqs. (10) admit an exponential solution $\overline{c^2} \sim \exp(-2\lambda/\beta t)$, $A \sim \exp(-2\lambda/\beta t)$, which means that the striation thickness δ remains constant at the latter stages of the mixing process. If $\beta=0$ the striation thickness scales as $\delta \sim \exp(-\lambda t)$ and the variation of the scalar decreases superexponentially as it is predicted by the lamellar model: $\overline{c^2} \sim \exp(-\lambda^{-1}\,\mathrm{Pe}^{-1}\delta^{-2})$.

The system of Eqs. (4) and (6)–(9) provides a closed description of the process. To perform the calculations we have to specify the artificial diffusion $\mathcal{D}$. We reject the simplest choice $\mathcal{D}=\mathrm{const}$ as introducing too high error in the solution. Note that the transport from the large to the subgrid scales takes place at the regions with high gradients of the concentration. It is also known that a numerical solution of Eq. (1) suffers from spurious oscillations at these regions and an extra diffusion is applied *locally* to keep the numerical scheme monotone [17]. Therefore, it is quite natural to combine these two tasks, i.e., we can solve Eq. (1) by a monotone scheme with an artificial diffusion and the artificial diffusivity of this scheme can be used to evaluate the transport of the scalar variance from large to subgrid scales. In the present investigation we use the flux-corrected transport (FCT) method described in the Ref. [17]. A one-dimensional advection equation $\partial_t \phi + U \partial_x \phi = 0$ is solved on a uniform grid with space increment Δx as follows.

(1) Compute a first-order upwind flux $Q_{i+(1/2)} = \max(U,0)\phi_i + \min(U,0)\phi_{i+1}$, then the low-order solution reads

$$\tilde{\phi}_i = \phi_i^0 - \frac{\Delta t}{\Delta x}[Q_{i+(1/2)} - Q_{i-(1/2)}]. \tag{11}$$

(2) Compute the second-order antidiffusive flux

$$Q^{ad}_{i+(1/2)} = \frac{1}{2}|U|(\phi_{i+1} - \phi_i). \tag{12}$$

(3) Limit the antidiffusion flux so that the solution, as computed in step 4, is free of the spurious oscillations

$$Q^c_{i+(1/2)} = \chi_{i+(1/2)} Q^{ad}_{i+(1/2)}.$$

(4) Apply the correction flux to get the new solution

$$\phi_i = \tilde{\phi}_i - \frac{\Delta t}{\Delta x}[Q^c_{i+(1/2)} - Q^c_{i-(1/2)}]. \tag{13}$$

Equations (11)–(13) have first-order accuracy in time and we use these equations to construct a fourth-order Runge-Kutta method. Thus, the numerical diffusion of the method is due to the finite-difference representation of the spatial derivative in the advection equation. Since the numerical diffusivity of Eq. (11) is $1/2U\Delta x$, the artificial diffusivity of Eqs. (11)–(13) is

$$\mathcal{D}_{xx,i+(1/2)} = \frac{1}{2}\chi_{i+(1/2)} U \Delta x. \tag{14}$$

Other components of the tensor $\mathcal{D}_{mn}$ can be calculated in the same way.

III. RESULTS AND DISCUSSION

In evaluating the models described above, we consider mixing by a (two-dimensional) model chaotic "sine flow" [18]. The flow takes place in a square box $0 \leqslant x, y \leqslant 1$ with sides $x=0$ and $x=1$ identified (so that fluid passing through one side reenters through the other), and similarly for the sides $y=0$ and $y=1$. The flow field is assumed to be time-periodic, with period T; then [18]

$$(u_x, u_y) = \begin{cases} (\sin 2\pi y, 0), & mT \leqslant t < \left(m + \frac{1}{2}\right)T \\ (0, \sin 2\pi x), & \left(m + \frac{1}{2}\right)T \leqslant t < (m+1)T \end{cases} \tag{15}$$

for $m=0,1,2,\ldots$. The initial state is given by

$$C(0,x,y) = \begin{cases} 1, & 0 \leqslant x < \frac{1}{2} \\ -1, & \frac{1}{2} \leqslant x < 1. \end{cases} \tag{16}$$

The case $T=1.6$ is "globally chaotic," i.e., there are no large nonchaotic islands in the flow, while for the lower values of period T the chaotic regions coexist with quasiperiodic ones.

In order to verify our results we use the similarity between the advection-diffusion equation (1) and Fokker-Plank equation of a diffusive process [19]. Linear functionals of the solution of Eq. (1) can then be estimated by a Monte Carlo method and the required computational resources do not depend on Pe, the details are given in the Appendix.

The performance of the method in the fully chaotic case $T=1.6$ is illustrated in Fig. 1. The Monte Carlo method predicts that after an initial period which depends (logarithmically) on Pe, C^2 decays exponentially. It follows from Eq. (10) that the slope of C^2 in Fig. 1(a) is $-2\lambda/\beta$. Since in this case the stretching rate $\lambda=1.2$, we are able to extract the parameter β from our Monte Carlo simulations. As one can see, β varies very slowly with Pe. The mechanism of mixing has two stages, at the first stage the variations of the scalar pass from the large to the subgrid scales. This process is mesh dependent; a fine mesh resolves more details of the concentration field and the scale-to-scale transport is slower, while the overall dissipation rate does not depend strongly on Δx. At the second stage C^2, which is mainly at the subgrid level, decays exponentially.

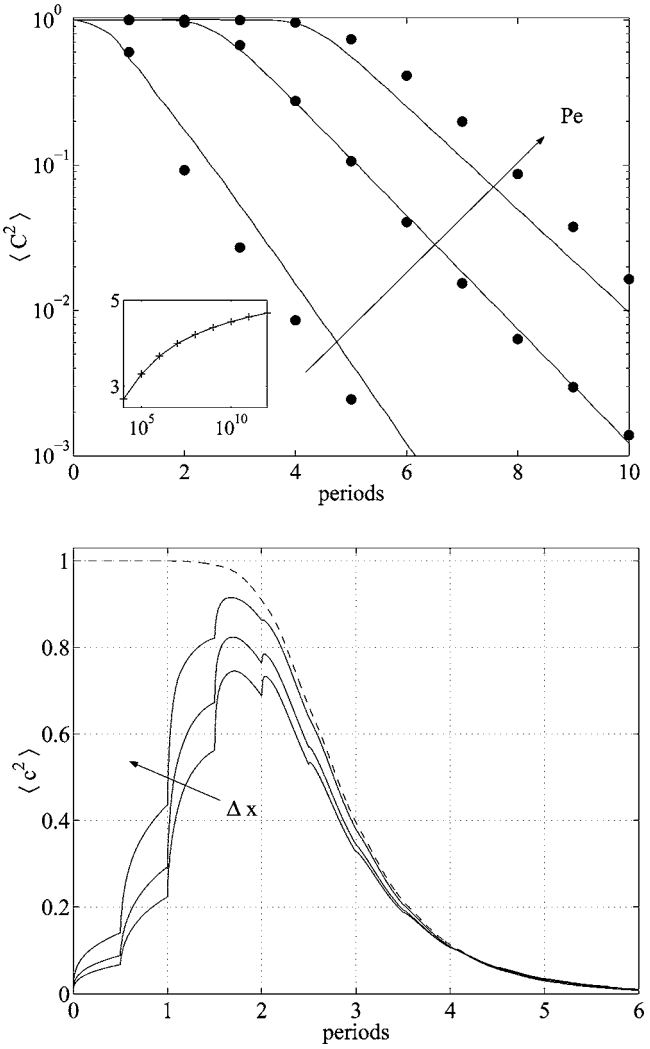

FIG. 1. Performance of the method: (a) $\langle C^2 \rangle$ as a function of time for Pe$=10^4$, Pe$=10^8$, Pe$=10^{12}$, and $T=1.6$ by the Monte Carlo method (symbols) and by the coarse-grained simulations (curves); (b) β as a function of Pe is shown on the insertion. $\langle c^2 \rangle$ as a function of time for $\Delta x=60^{-1}$, $\Delta x=120^{-1}$, $\Delta x=180^{-1}$, Pe$=10^8$, and $T=1.6$. The time evolution of $\langle C^2 \rangle$ is shown by a dashed line.

The fully chaotic case is very simple for analysis. Since the system is well mixed, even the zero-dimensional model (10) captures the main features of the process. A more interesting test case is when $T=1.0$ and the chaotic region coexists with nonchaotic islands. The process consists of three

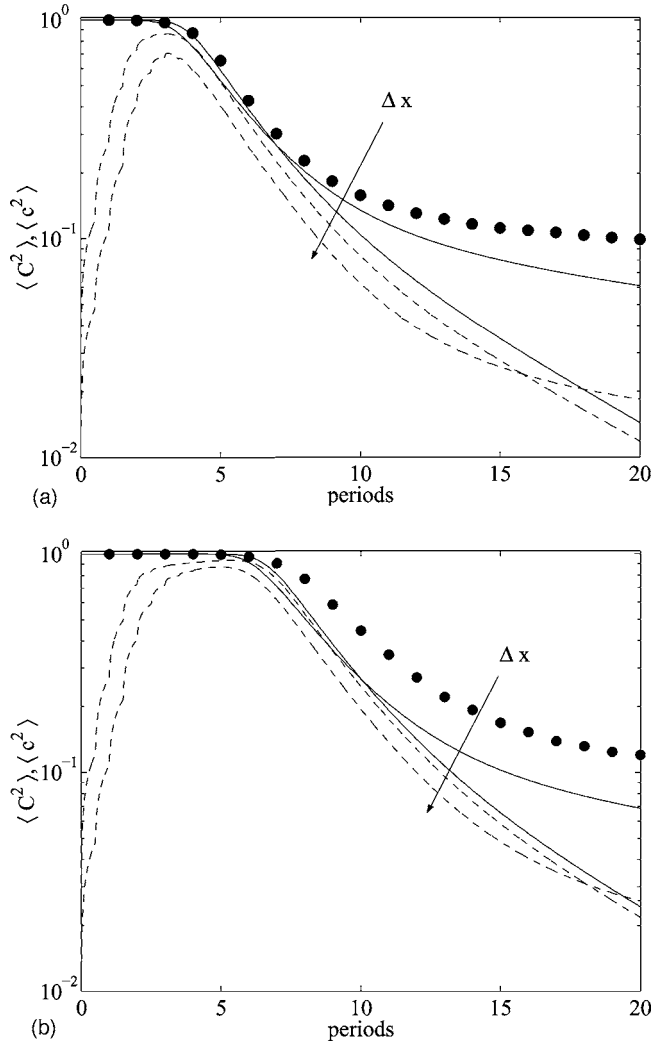

FIG. 2. $\langle C^2 \rangle$ as a function of time for the semichaotic case $T=1.0$ by the Monte Carlo method (symbols) and by the coarse-grained simulations (curves) for $\Delta x=60^{-1}$ and $\Delta x=240^{-1}$, respectively; $\langle c^2 \rangle$ is shown by dashed lines; β is the same as in Fig. 1(a). (a) $\mathrm{Pe}=10^8$, (b) $\mathrm{Pe}=10^{12}$

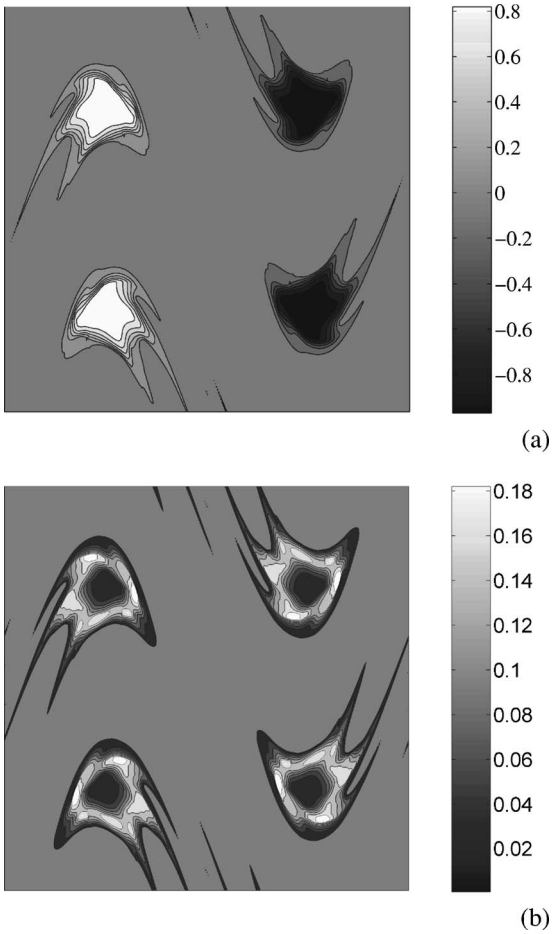

FIG. 3. (a) C and (b) c^2 after 20 periods of mixing for semichaotic case $T=1.0$; $\mathrm{Pe}=10^{-12}$ and $\Delta x=240^{-1}$.

stages as it is shown in Fig. 2. Initially variations of the concentration are transported to the subgrid scales in the chaotic region, but no dissipation occurs at this stage. When the characteristic striation thickness becomes small enough, the diffusion leads to fast dissipation in the chaotic region. At the third stage the mixing rate drops down and "dissolving" of the laminar island becomes the rate-limiting process. At this stage the accuracy of the predictions depends on the ability of the method to resolve the nonchaotic regions properly. As it is demonstrated in Fig. 2, a coarse mesh overestimates the mass transfer from the laminar islands and mesh refinement is necessary to achieve a reasonable agreement between the predictions of the method and the results of the Monte Carlo simulations.

Figure 3 shows C and c^2 after 20 periods of the mixing. As we can see, the subgrid variation of the scalar concentration is low in the chaotic region (due to the intensive mixing) and inside the laminar islands (due to the total lack of the mixing). The scale-to-scale transport occurs in a thin layer at the boundary of the laminar island and the precision of the method depends on the proper resolution of this layer. Since the artificial diffusivity increases the thickness of the interface and overestimates the mass flux across the boundary, it is of crucial importance to keep the scheme diffusivity as low as possible.

IV. CONCLUSIONS

We have proposed and tested an approximate method for the simulation of chaotic mixing with high Péclet numbers on coarse grids. The method adopts the ideas which have been used in the simulation of turbulent flows, namely direct resolution of large scales which then transfer variation of the scalar to the subgrid scales as in large-eddy simulations. The subgrid scales are modeled through mean field variables: the coarse-grained mixedness c^2 and tensor $A_{ij}=\partial c/\partial x_i \partial c/\partial x_j$, i.e., the proposed method is very similar to the k-ϵ model of turbulence. While in turbulent flows the transport of the kinetic energy to the subgrid scales is done by a turbulent viscosity, in the present model we use a purely numerical artefact, the scheme diffusion. Each time the finite volume method cannot resolve the profile of the concentration, the solution is spread over nearby control volumes and the corresponding amount of mixedness is added to the subgrid

level. The analogy with turbulent flows modeling can be extended to chaotic mixing with chemical reactions. Since the dissipation rate A_{kk} which is explicitly tracked by the proposed method plays a central role in flamelet and conditional moment closure (CMC) models of turbulent combustion [20,21], a similar approach can be incorporated in the proposed model of chaotic mixing.

The method works reasonably well in the chaotic region. In order to be able to predict mixing in real situations, the method has to resolve the thin layer at the boundary between laminar and chaotic regions properly. Since the method used in the present investigation, namely, first-order upwind predictor and second-order central differences corrector has a high scheme diffusion, use of more advanced higher-order WENO schemes [22] should improve the performance of the method.

APPENDIX: MONTE CARLO METHOD FOR ESTIMATION OF THE QUALITY OF THE MIXING

We use the similarity between the advection-diffusion equation (1) and Fokker-Plank equation of a diffusive process [19]. Linear functionals of the solution of Eq. (1) can then be estimated by a statistical simulation Monte Carlo method and the required computational resources do not depend on Pe. If one considers Eq. (1) as the forward Kolmogorov or Fokker-Planck equation of a stochastic process [here we use the fact that $\partial_{x_k} u_k = 0$ and u_k in Eq. (1) can be taken out of the divergence operator], the backward Kolmogorov equation of the same process reads

$$\frac{\partial C}{\partial \tau} - u_k \frac{\partial C}{\partial x_k} - \frac{1}{\mathrm{Pe}} \frac{\partial^2 C}{\partial x_k^2} = 0, \tag{A1}$$

where $\tau = -t$ is backward directed time. In order to calculate the quality of the mixing in a point $\boldsymbol{x}^0$ at a time t we track a tracer particle backward in time according to the stochastic differential equation that corresponds to Eq. (A1),

$$dx_i(\tau) = -u_i(\tau, x_l)d\tau + \sqrt{2/\mathrm{Pe}}\, dW_i, \quad x_i(t) = x_i^0, \tag{A2}$$

where dW_i is the increment of a Wiener process with unit dispersion. The concentration at the point $\boldsymbol{x}^0$ can be estimated by the Monte Carlo method as $C(\boldsymbol{x}^0) = \langle \xi \rangle$, where

$$\xi = 1, \qquad \boldsymbol{x}(0) \in \Omega_1,$$
$$\xi = -1, \qquad \boldsymbol{x}(0) \in \Omega_2,$$

and $\langle \cdot \rangle$ means mathematical expectation. Ω_1 denotes the subsets of the domain Ω where the scalar is initially placed, $\Omega_2 = \Omega \backslash \Omega_1$.

Consider two statistically independent diffusion trajectories which start at the point $\boldsymbol{x}^0$ at the same time. Since they are independent

$$\langle \xi_1 \xi_2 \rangle = \langle \xi_1 \rangle \langle \xi_2 \rangle = C^2(\boldsymbol{x}^0). \tag{A3}$$

Thus, only two random trajectories suffice in order to obtain an *unbiased* Monte Carlo estimate for the variation of the concentration at a point. The estimation (A3) can be extended to the case of n independent trajectories

$$C^2(\boldsymbol{x}^0) = \left\langle \frac{2}{n(n-1)} \sum_{i=1, j=i+1}^{n-1, n} \xi_i \xi_j \right\rangle. \tag{A4}$$

It can be shown that the random error of the estimate (A4) decreases approximately by factor 2 when n increases to 15 and then decreases slowly as $n \to \infty$.

Therefore, the Monte Carlo algorithm for the calculation of $\langle C^2 \rangle$ reads as follows:

(1) Generate a uniformly distributed point $\boldsymbol{x}^0$.

(2) Track a random trajectory (A2) with the initial conditions $\boldsymbol{x}^0$.

(3) Repeat step 2 n times and estimate $C^2(\boldsymbol{x}^0)$ according to Eq. (A4).

(4) Repeat steps 1–3 N times ($N \gg 1$) and average the results obtained.

[1] H. Aref, J. Fluid Mech. **143**, 1 (1984).
[2] J. M. Ottino, *The Kinematics of Mixing: Stretching, Chaos and Transport* (Cambridge University Press, 1989).
[3] H. Aref, Phys. Fluids **14**, 1315 (2002).
[4] H. A. Stone, A. D. Strook, and A. Ajdari, Annu. Rev. Fluid Mech. **36**, 381 (2004).
[5] F. J. Muzzio and J. M. Ottino, Phys. Rev. A **40**, 7182 (1989).
[6] F. J. Muzzio and J. M. Ottino, Phys. Rev. A **42**, 5873 (1990).
[7] J. M. Ottino, Chem. Eng. Sci. **49**, 4005 (1994).
[8] X. Z. Tang and A. H. Boozer, Physica D **95**, 283 (1996).
[9] X. Z. Tang and A. H. Boozer, Phys. Fluids **11**, 1418 (1999).
[10] X. Z. Tang and A. H. Boozer, Chaos **9**, 183 (1999).
[11] J.-L. Thiffeault, Phys. Lett. A **309**, 415 (2003).
[12] J.-L. Thiffeault and A. H. Boozer, Chaos **11**, 16 (2001).
[13] M. Lesieur and O. Métais, Annu. Rev. Fluid Mech. **28**, 45 (1996).
[14] C. Meneveau and J. Katz, Annu. Rev. Fluid Mech. **32**, 1 (2000).
[15] A. Celani, M. Martins Afonso, and A. Mazzino, http://fr.arXiv.org/abs/http://fr.arxiv.org/abs/nlin.CD/0602061, 2006.
[16] O. S. Galaktionov, P. D. Anderson, G. W. M. Peters, and Charles L. Tucker III, Int. J. Multiphase Flow **28**, 497 (2002).
[17] E. S. Oran and J. P. Boris, *Numerical Simulation of Reactive Flows* (Elsevier Science, New York, 1987).
[18] J. G. Franjione and J. M. Ottino, Philos. Trans. R. Soc. London, Ser. A **338**, 301 (1992).
[19] A. Vikhansky, Phys. Fluids **12**, 4738 (2004).
[20] R. O. Fox, *Computational Model for Turbulent Reaction Flows* (Cambridge University Press, Cambridge, 2003).
[21] A. Y. Klimenko and R. W. Bilger, Prog. Energy Combust. Sci. **25**, 595 (1999).
[22] X. D. Liu, S. Osher, and T. Chan, J. Comput. Phys. **115**, 200 (1994).